Dundee Discussion Papers in Economics 267

Chen, Yu-Fu; Funke, Michael

Publication date:
2012

Dundee Discussion Papers
in Economics

GLOBAL WARMING AND FAT TAILED-UNCERTAINTY: RETHINKING THE TIMING AND INTENSITY OF CLIMATE POLICY

Yu-Fu Chen & Michael Funke

Department of
Economic Studies
University of Dundee
Dundee
DD1 4HN

Working Paper
No. 267
June 2012
ISSN: 1473-236X

GLOBAL WARMING AND FAT TAILED-UNCERTAINTY: RETHINKING THE TIMING AND INTENSITY OF CLIMATE POLICY

Yu-Fu Chen

University of Dundee
Economic Studies
Dundee DD1 4HN
UNITED KINGDOM
Email: y.f.chen@dundee.ac.uk

Michael Funke

Hamburg University
Department of Economics
Von-Melle-Park 5
20146 Hamburg
GERMANY
Email: funke@econ.uni-hamburg.de

Dundee & Hamburg, Revised June 2012

Abstract

The possibility of low-probability extreme natural events has reignited the debate over the optimal intensity and timing of climate policy. In this paper, we contribute to the literature by assessing the implications of low-probability extreme events on environmental policy in a continuous-time real options model with "tail risk". In a nutshell, our results indicate the importance of tail risk and call for foresighted pre-emptive climate policies.

Acknowledgement

The research was supported through the Cluster of Excellence "Integrated Climate System Analysis and Prediction" (CliSAP), University of Hamburg, and funded through the German Science Foundation (DFG). An earlier version of the paper has been presented at the Annual Conference of the Royal Economic Society at Royal Holloway, University of London (18-20 April 2011). We would like to thank various participants for helpful comments and suggestions. The usual disclaimer applies.

Keywords: Climate Policy, Extreme Events, Real Options, Levy process
JEL-Classification: D81, Q54, Q58

1. Introduction

The term extreme event refers to infrequent weather and natural events that deviate significantly from the norm. Scientists cannot state with confidence that today´s extreme events are the first signs of climate change arising from greenhouse gas (GHG) emissions. Nevertheless, the monitoring and studying of extreme events, and learning how to cope with them, must be a priority. Global climate change could well affect the frequency, magnitude and location of extreme events. Extreme weather events that may be considered here include droughts (due to increased evaporation and reduced precipitation), river floods (due to increased precipitation), landslides (due to increased precipitation), Storms, cyclones and tornadoes (due to changing heat transport patterns and increased land-ocean temperature differential), and ocean and coastal surges and related flooding (due to storms and sea level rise). Any shift in average climatic conditions will almost inevitably boost the frequency of these extreme events - some of these changes are already occurring - and traditional diversification strategies may fail. Extreme climate events are different from other shocks because their impacts are persistent for many years or even permanent. Therefore extreme event research can be regarded as an interdisciplinary issue that cuts across a multitude of research fields.[1]

The occurrence of an extreme event, however, does not automatically imply a prolonged impact upon economies. Apart from the obvious situation where an event occurs in an uninhabited area, impacts will vary depending notonly on the location in which it occurs but also on spatial and temporal dimensions and the population and wealth at risk. It is, however, likely that extreme events will have an increasing effect on human well-being in future decades. Because the most affected countries in the tropics are poor, those most likely to be affected will be least able to adapt. On the other hand, the colder parts in the northern hemisphere may benefit from climate change, but they too face perils.[2]

Consequently, critics of policies to reduce GHG emissions vigorously question whether policymakers should address these issues now, given that the monitoring of extreme event impacts is fraught with difficulties. These issues have sparked considerable debate in recent times. Do non-negligible low-probability tail risks call for an early and significant environmental policy action? How much should we invest now in exchange for benefits in the distant future? What is the appropriate vigour of policy responses in the face of extreme, abrupt climate-change scenarios? This paper tries to come to grips with problems of this type. To place this analysis in context, it is useful to distinguish second-order uncertainty (thin-tail uncertainty) from higher-moment uncertainty (fat-tail uncertainty). Second-order

[1] Valdez (2011) has argued that complex natural science climate models are at their limit when modelling extreme events and abrupt climate changes. If anything, climate models tend to underestimate past climate changes, compared to geological record. Climate simulations of the coming century may therefore give us a false sense of security.

[2] The Intergovermental Panel on Climate Change (IPCC, 2007) and the Stern (2007) report have indicated that global warming will cause an increase in the frequency and severity of extreme weather events and natural disasters. Webster et al. (2005) and Hoyos et al. (2006) have shown that the number, duration, and intensity of hurricanes are highly correlated with temperature. See Weitzman (2009) for a recent discussion of catastrophic risks from climate change and references to the literature on this issue.

uncertainty examines the impact of the second moment of the distributions assuming that the distributions are normal or at least close to normal. Assumptions based on the impact of second-order uncertainty is the "industry standard" in the real options literature. In contrast, higher-moment uncertainty emphasises the issue of fat tails in the distribution of certain parameters and the risk of catastrophic climate change.

Recent advances in theory have made real option valuation techniques applicable to a multitude of real world situations. A general discussion on real options can be seen from growing literature such as Dixit and Pindyck (1994), Stokey (2008), and Chevalier-Roignant et al (2011). Following the growing adaption of fat-tailed stochastic processes in derivatives pricing, extreme events are also used to in real options. e.g. Martzoukos and Trigeorgis (2002) use multiple sources of extreme events to discuss the pricing of real options. In climate change research, Pindyck´s (2000) uses options-based model of irreversible investment to evaluate the thresholds of optimal environmental policy for greenhouse gas emission. For a brief survey of the real options approach in environmental economics, see Pindyck (2007, pp. 58-59). In this paper, we use a standard Levy process to discuss damage thresholds of the environmental policy for various possible changes in temperature scenarios.

The layout of the paper is as follows. In section 2 we develop a continuous-time real option model of climate policy with "tail risk" addressing the complexities of climate change interactions and their challenging policy implications. The real option tool is widely used and very valuable in identifying and describing choices under uncertainty and irreversibility. Uncertainty and irreversibility are central to environmental policies. First, uncertainty surrounds the underlying climatological, geophysical, and hydrological processes. These uncertainties are exacerbated by uncertainty over the exact environmental damage, as well as uncertainty with regard to what technological progress might be required to ameliorate those environmental damages in the future. Second, climate patterns are partly irreversible, i.e. they cannot be reversed. Section 3 contains an in-depth numerical analysis and interpretation of our results. The final section of the paper summarizes some key findings and draws out some brief policy implications. Technical details and derivations are presented in the appendices.

2. A Real Options Model of Irreversible Investment with Low-Probability Extreme Events

Against this background, we develop an options-based model of irreversible investment incorporating extreme events. This adds yet another layer of complexity to the climate policy debate.[3] Suppose that risk-averse policymakers is maximise the welfare function

[3] Note that Baranzili et at (2003) have used a simple jump process, combined with a mean-reverting stochastic process or geometrical Brownian motion, to discuss the fat tail - climate policy nexus in a real option setup. However, their discussions are limited with respect to a stochastic process with a simple constant jump size. In contrast, we use a Levy process to discuss the impact of extreme events upon climate policy probabilistically with a spectrum of different jump sizes, generated from compound Poisson jumps.

(1) $$W = E\left[(1-w)\int_0^{\infty}\left(1-D(\theta_t,T_t)\right)Y_t e^{-rt}dt\right] = E\left[(1-w)\int_0^{\infty}\left(1-k\theta_t^{\mu}T_t^2\right)Ye^{-(r-\eta_Y)t}dt\right],$$

where $E[\ ]$ is the expectation operator, r is the discount rate, Y_t represents the output or consumption over time, T_t is changes in temperature since the pre-industry era, $D(\theta_t,T_t)$ is the damage function relative to Y_t, θ_t is the stochastic damage index with $\mu > 1$ and $k > 0$, and w is the mitigation expenses necessary to keep the future temperature increase within a predetermined threshold.

It is natural to assume that the damage ratio function is positively related to both the changes in temperature, T_t, and damages from extreme events due to climate change, θ_t.[4] Following Weitzman (2009), the change in temparature is modelled as

(2) $$dT_t = m_1\left(\frac{\ln\left(M_t / M_p\right)}{\ln 2} - m_2 T_t\right)dt,$$

where M_p is the inherited pre-industrial level of greenhouse gas, and m_1 and m_2 are positive parameters. Assume a doubling of the atmospheric greenhouse gases $M_t = 2M_p$. Equation (2) is then reduced to $dT_t = m_1\left(1-m_2T_t\right)dt$. It is obvious that as time approaches infinity, changes in temparature reach the final equilibrium level $T_{\infty} = 1/m_2$. Let H denote the half-time needed to reach the equilibrium change in temparature. Then we have $2T_H = 1/m_2$ and $T = T_H$ at $t = H$. It is straightforward to see that the process of T has the following solutions

(3) $$T_t = e^{-\frac{\ln 2}{H}t}\left(T - 2T_H\left(1-e^{\frac{\ln 2}{H}t}\right)\right),$$

where $T = T_0$ at $t = 0$; $T_{\infty} = 2T_H$; $T_t = T_H$ at $t = H$ with assumption $T = 0$; and equation (3) satisfies $dT_t = m_1\left(1-m_2T_t\right)dt$ with $1/m_2 = 2T_H$ and $m_1 = 2\frac{\ln 2}{H}T_H$. Equation (2) then simplifies to

[4] In the climate change literature, e.g Weitzman (2010), the damage function is usually assumed to be convex to changes in temperature: $d(D/dT) > 0$ and $d^2(D/dT^2) > 0$. We choose a simple quadratic function with respect to T for the policymaker. This is consistent with the climate sensitivity estimates reported in Maslin and austin (2012). The damage function $k\theta_t^{\mu}T_t^2$ is also a first-order approximation of the exponential damage function $\left(1-\exp\left(-k\theta_t T_t^2\right)\right)$, which gives $k\theta_t T_t^2$ by Taylor series expansion. The exponential damage function naturally gives the property of risk-averseness; hence, we add parameter μ to our damage function. As the climate damage relative to the GDP is relatively small, one can consider the first-order Taylor series expansion to be a good approximation.

(4) $$dT_t = \frac{\ln(2)}{H}\left(2T_H - T_t\right)dt,$$

Equations (4) is an essential building block in the real options modelling setup, while equation (3) is useful for directly integrating the intertemporal climate change damage function. We later use equation (3) to compute the integral directly by setting current temparature change since the pre-industry era to be $T = 0.6$.

Therefore, the next step is to model the underlying uncertainty. In prototypical real option models a Gaussian structure for the shocks is usually assumed. However, the evidence presented above suggests that climate change is better described by distributions with fat tails. A heavy-tailed distribution attaches a higher probability to extreme events than normal distribution. There are many stochastic processes of heavy-tailed distributions used in finance. Among them is the commonly used Levy process which has independent and stationary increments. The Levy process treats extreme events probabilistically and is simultaneously fairly general and analytically tractable. Many continuous-time stochastic processes are special cases of the general Levy processes, such as the Brownian motion, and Poisson processes. In this paper, we use one-side compound Poisson jumps, combined with a Brownian motion, to model potential sudden swings (large kurtosis and skewness) of global/local social/environmental damage, caused by more frequent extreme events from GHG-induced climate changes. Broadly speaking, the compound Poisson processes in a Levy process show independent random variables with the same intensity as dictated by comparable Poisson processes, but the jump sizes of the random variables are independent and identically distributed with a Levy density. This means that by utilising different parameter values of a Levy density, we can model different types and intensities of extreme events.[5]

The fat-tailed Levy process X_t with characteristic triplet $\left(\sigma^2, \nu, \gamma\right)$ takes the form of the Levy-Khinchin representation (see, e.g., Sato (1999); Cont and Tankov (2004))

(5) $$E\left[e^{izX_t}\right] = \exp\left[t\left(-\frac{\sigma^2 z^2}{2} + i\gamma z + \int_{-\infty}^{\infty}\left(e^{izx} - 1 - izx\mathbf{1}_{|x|\le 1}\right)v(dx)\right)\right],$$

where σ is a positive real number, γ is a constant, and ν is a measure of the jump intensity with jump size x, satisfying $\int_{-\infty}^{\infty} x^2 v(dx) < 0$ and $\int_{|x|>1} v(dx) < \infty$. The stochastic process X can then be interpreted as a drifted Brownian motion combined with an independent compound Poisson process with jump

[5] Rachev (2003) reviews the research on heavy tailed distributions in finance. Among others, further recent papers include Duffie et al. (2000), Cont and Tankov (2004), Kou and Wang (2004), Oksendal and Sulem (2007), and Schoutens (2007).

probability $\lambda = \int v(dx)$ and $v(dx)$ is the Levy measure. In addition, the corresponding Levy infinitesimal generator of the Levy process X has the form

$$
\begin{aligned}
L^X f(x) &= \lim_{\Delta t \to 0} \frac{E\left[f(x + X_{\Delta t}) - f(x) \right]}{\Delta t} \\
&= \frac{\sigma^2}{2} \frac{\partial^2 f}{\partial x^2} + \gamma \frac{\partial f}{\partial x} + \int_{-\infty}^{\infty} \left(f(x+y) - f(x) - y \mathbf{1}_{|y| \le 1} \frac{\partial f}{\partial x}(x) \right) v(dy).
\end{aligned} \tag{6}
$$

For an exponential Levy process $\theta_t = \exp(X_t)$, we then have the following integro-differential Bellman equation by applying Ito-Levy lemma, as shown in Cont and Tankov (2004) and Schoutens (2003):

$$
\begin{aligned}
(r - \eta_Y) W &= (1-w)\left(1 - k\theta^{\mu} T^2\right) + \frac{\ln 2}{H}(2T_H - T) W_M \\
&\quad + \alpha \theta W_{\theta} + \frac{1}{2}\sigma^2 \theta^2 W_{\theta\theta} + \int_{-\infty}^{\infty} \left[W\left(\theta e^{y}\right) - W(\theta) \right] \nu(dy),
\end{aligned} \tag{7}
$$

where partial derivatives are denoted by subscripts. Below we assume a constant aggregate drift parameter α.[6] Furthermore, Y is normalised to one. The meaning of the Levy process θ can be explicitly explained as an equivalent geometric Brownian motion with compound Poisson jumps, which also yields Bellman equation (7),

$$
d\theta_t = \alpha \theta_t dt + \sigma \theta_t dz_t + \theta_t \sum_{i=1}^{N_t} J_i , \tag{8}
$$

where z is the standard Wiener process, and $\sum_{i=1}^{N_t} J_i$ is a (memoryless) compound Poisson process with intensity $\lambda > 0$. Each of the jump sizes is i.i.d., and N_t is a Poisson process with intensity λ, independent from $(J_i)_{i \ge 1}$. The compound Poisson processes in a Levy process show independent random variables with the same intensity of the same Poisson process, but the jump sizes of random variables are independent and identically distributed with a Levy density. This means that we can model different extreme events via different parameter values of the Levy density. Note that the Brownian motion part does not enter the Levy measure and both are independent from each other.

Furthermore we assume that the Levy measure has the one-sided density measure $\nu(y) = \lambda f(dy) = \lambda \eta e^{-\eta y} dy, \ = \lambda \eta e^{-\eta y} dy, \ y > 0$. Therefore, equation (7) can be rearranged to show

[6] Note that $\alpha = \gamma + \int \left(1 - e^{y}\right) v(dy)$ corresponds to the α parameter in Pindyck (2000).

$$(9)\qquad \begin{aligned}(r-\eta_Y)W &= (1-w)\left(1-k\theta^{\mu}T^{2}\right)+\frac{\ln 2}{H}\left(2T_H-T\right)W_T+\alpha\theta W_{\theta}\\ &\quad+\frac{1}{2}\sigma^{2}\theta^{2}W_{\theta\theta}+\lambda\int_0^{\infty}\left[W\left(\theta e^{y}\right)-W\left(\theta\right)\right]\eta e^{-\eta y}dy.\end{aligned}$$

The one-sided jumps – the same Levy density definition as in Kou and Wang (2004) – have two positive parameters of the Levy measure, λ and η, which show the overall probability of such jump events occurring and the distributions of such jump events over *y*, respectively. It is straightforward to see that for smaller the values of η, the extreme events in terms of higher values of *y* are occurring more often. Below we shall see that these two parameters substantially affect the climate policy implications.

The policy maker faces a binary optimal stopping problem. Choosing no action in a business-as-usual scenario yields the no action welfare W^{N} with $w = 0$. On the contrary, if the policymaker adopts a credible environmental policy, a certain temperature target $T_H \le \tau$ is assumed to be met after H years by paying a fixed *w* percentage of output to reduce emission providing welfare of action W^{A}. We show in Appendix A that the welfare for no action (business-as-usual case) W^{N} and the welfare of taking action W^{A} have the following solutions, if no real options are considered.

$$(10)\qquad W^{\mathrm{N}}=\frac{1}{\left(r-\eta_Y\right)}-k\left[\frac{\left(2T_H-T\right)^{2}}{\phi_1+2\frac{\ln 2}{H}}-\frac{4T_H\left(2T_H-T\right)}{\phi_1+\frac{\ln 2}{H}}+\frac{4T_H^{2}}{\phi_1}\right]\theta^{\mu},$$

$$(11)\qquad W^{\mathrm{A}}=(1-w)\left(\frac{1}{\left(r-\eta_Y\right)}-k\left[\frac{\left(2\tau-T\right)^{2}}{\phi_1+2\frac{\ln 2}{H}}-\frac{4\tau\left(2\tau-T\right)}{\phi_1+\frac{\ln 2}{H}}+\frac{4\tau^{2}}{\phi_1}\right]\theta^{\mu}\right),$$

where $\phi_1 = r-\eta_Y-\mu\alpha-\frac{1}{2}\mu(\mu-1)\sigma^{2}-\frac{\lambda\mu}{\eta-\mu}>0$ and T_H is replaced by τ.

To derive the optimal investment rule using dynamic programming, the value-matching condition has to be satisfied. The value-matching condition indicates that the marginal benefit value is equal to the marginal value of waiting or real options W^{O}. The marginal value of investing or benefit from a credible climate policy is represented by $W^{\mathrm{A}}-W^{\mathrm{N}}$. Thus, we have the value-matching condition,

$$(12)\qquad F(T)\bar{\theta}^{\mu}=\frac{w}{\left(r-\eta_Y\right)}+W^{\mathrm{O}}\left(T,\bar{\theta}\right),$$

where

$$F(T)=k\frac{\left(2T_H-T\right)^2-(1-w)(2\tau-T)^2}{\phi_1+2\frac{\ln 2}{H}} - k\frac{4T_H\left(2T_H-T\right)-4(1-w)\tau(2\tau-T)}{\phi_1+\frac{\ln 2}{H}}+k\frac{4T_H^2-4(1-w)\tau^2}{\phi_1} \tag{13}$$

where W^{O} denotes real options, $\bar{\theta}$ is the threshold where the society exercises its option to adopt the climate policy, i.e. for $\theta>\bar{\theta}$, it is optimal to adopt the GHG-cutting policies. $F(T)$ is positive (see Appendix A for details). The term $F(T)\bar{\theta}^{\mu}$ denotes the benefit of adopting the policies of reducing GHG and temperatures while the term $wY/(r-\eta_Y)$ gives the intertemporal value of (future) sunk cost from the credible climate policy as the policy maker pays *w* every year.

It is well-known that analytical solutions for jumps to a pre-jump-state-dependent state outside the continuation region are difficult to obtain. We therefore compute the real option values W^{O} and the thresholds $\bar{\theta}$ numerically. We employ a standard explicit finite difference method, and the discretisation method of the Level jump integral is similar to Cont and Voltchkova (2005). In addition to the value-matching condition (13), the numerical solutions need to satisfy the following boundary conditions:

$$W^{\mathrm{O}}(\theta=0,T)=0, \tag{14}$$

$$\lim_{\theta\to\infty}W^{\mathrm{O}}(\theta,T)=\lim_{\theta\to\infty}\max\left(W^{\mathrm{A}}(\theta,T)-W^{\mathrm{N}}(\theta,T),0\right), \tag{15}$$

$$W^{\mathrm{O}}(\theta,T_{\mathrm{Max}})=\left(W^{\mathrm{A}}(\theta,T_{\mathrm{Max}})-W^{\mathrm{N}}(\theta,T_{\mathrm{Max}}),0\right). \tag{16}$$

Equations (14) and (15) are straightforward as we expect that a zero value of θ gives zero real option value, while a large value for θ will lead to an immediate exercise of the real option. The terminal condition for *T* needs to be handled with care. We assume that the policymaker will exercise the real option once *T* is approaching $T_{\max}=\tau$, whereby $T_{\max}>\tau$ means that it is too late to adopt an effective climate policy. The $\bar{\theta}$ thresholds are obtained after backward computation $T=T_{\max}=\tau$ to $T=0.6$, the current changes in temperature relative to pre-industrial level, by an explicit finite difference method (see Appendix B for further computational details). Once we have obtained the thresholds $\bar{\theta}$, we can compute the damage thresholds $\bar{D}$ as

$$\bar{D}=k\bar{\theta}^{\mu}T^2=0.36k\bar{\theta}^{\mu}, \tag{17}$$

assuming that current T is 0.6 degrees higher than in the pre-industrial era.

The model presented above frames the economic analysis of highly uncertain extreme climate events. This provides the platform for the numerical analysis that allows us to solve the optimal stopping problem and solve for the optimal intensity and timing of policy responses.

4. Model Simulations

Section 3 has provided a detailed presentation and discussion of the main features of the model. As we do not have the closed-form solutions for real options, we need to use extensive numerical illustrations to gain further insight into the results of the previous section in order to get an intuitive "feel" for the model. The most important goal of these simulations is to see how certain crucial aspects of the model react to changes in parameters. In order to simulate the model, we need to cross the "minefield" of calibration. As methodological issues related to calibration are not the focus of this paper, a pragmatic stance is taken.

The benchmark values for parameters are r = 0.035, $\alpha = 0.0$, $\sigma = 0.2$, T = 0.6, H = 100, $\tau = 2.0$.[7] The baseline parameter for μ in our global analysis is set to 1.2.[8] Furthermore we assume $\mu = 1.2$, $\eta_Y = 0.0$, k = 1/1000. The costs for mitigation costs are 2 per cent of worldwide GDP such that $w = 0.02$.

The calibration of the one-sided positive exponential compound jump distribution for extreme events needs some further consideration. As pointed out by Cont and Tankov (2004, Table 4.3), the probability density function of a Brownian motion with exponential compound jumps is not available in closed form. Therefore, we have to approximate the continuous probability density function (8) using discrete subsamples. In particular, we focus on the ranges for the values of λ and η. The exponential distribution of compound jumps, $\eta e^{-\eta y}$, implies that when jumps occur, most jumps are small, but sometimes the jumps become much larger, depending on the value of parameter η and λ. Last but not least, the choice of η and λ is made more difficult by the limited information about extreme event probabilities and their economic impact. Integrated assessment models yield a rough consensus that for mean temperature increases up to 4º C relative to today's temperature, the most likely impact is from 1 per cent to 5 per cent of GDP. Little is known about the outer tail of the distribution, but there is a real chance, substantiated by recent studies, that temperature increases of 3º C or 4º C could have a much

[7] The deterministic trend term α has been assumed to be zero without loss of generality. It may reflect the fact that the recent increase in temperature may be a transient phenomenon in a cyclical process that has no overall long-term trend. For example, a local upswing in an interdecadal sine wave may appear to be a trend when viewed in isolation.

[8] What is most certain is that the poorest countries in the developing world will be least able to adapt to any increase in the frequency and magnitude of extreme weather phenomena. Weitzman (2009) has demonstrated that in some regions extreme events may lead to very low consumption levels. This implies that welfare losses in those regions become large, and potentially unbounded. In a global analysis those results for a few regions are averaged

larger impact, as high as 8-10 per cent of GDP.[9] Below we assume that the benchmark value for the jump probability λ is equal to 6 per cent. We then determine a suitable range of η parameters such that the extreme event probabilities of different jump sizes are in the right order of magnitude.

As no analytical lognomal probability distribution function is available for θ in equation (8), we numerically simulate the probability density distribution of θ. The technical details of the numerical procedure are discussed below. Formally, equation (8) can be proxied by the Euler scheme

$$(18) \qquad \theta_{t+\Delta t} = \theta_t + \alpha\theta_t\Delta t + \sigma\theta_t\varepsilon_t\sqrt{\Delta t} + \theta_t\sum_{i=1}^{N} J_i\,, \qquad \varepsilon_t \sim N(0;1)\,,$$

where J_t is simulated from the exponential distribution of $\eta e^{-\eta y}$.[10] The intuition behind (18) exactly parallels that of its continuous-time counterpart (8). The distribution of the jumps is proxied by −ln(uniform distribution of [0,1])/η. This implies that the frequency of extreme events ranges from several years to decades or more.

In addition to providing some important intuition behind our results, equation (18) also delivers another important point. The extreme events are governed by the parameters η and λ. Indeed, smaller jumps happen more often for higher value of η. Conversely, greater disasters happen more often for smaller value of the parameter η. Technically, in the numerical simulations we pick 1 million random samples of (18) for θ_t with initial values $\theta_0 = 20$, σ = 0.2, λ = 0.06, and $\Delta t = 0.01$, and each realisation for θ is calculated for 10 years. The calibrated results in Figure 1 show distinctively that the lognormal probability distribution function depends upon which η parameter is at work. The left-hand side graph assumes η = 10 and the right-hand side graph uses η = 5.

---

out, but with a regional focus, these fat tails in single regions may drive the analysis. Below we therefore provide a sensitivity analysis with respect to μ.

[9] For a recent overview of concurrent studies, see Tol (2009). A graphical summary of damage estimates is provided by Dietz and Stern (2008).

[10] The sequential times of Poisson jumps are proxied by −ln(uniform distribution of [0,1])/λ. Therefore, when a Poisson jump happens, θ increases by $\theta_t\left(e^{Y_i} - 1\right)$.

Figure 1: Probability Density Distributions of θ for λ = 0.06 and η = 10 vs. η = 5

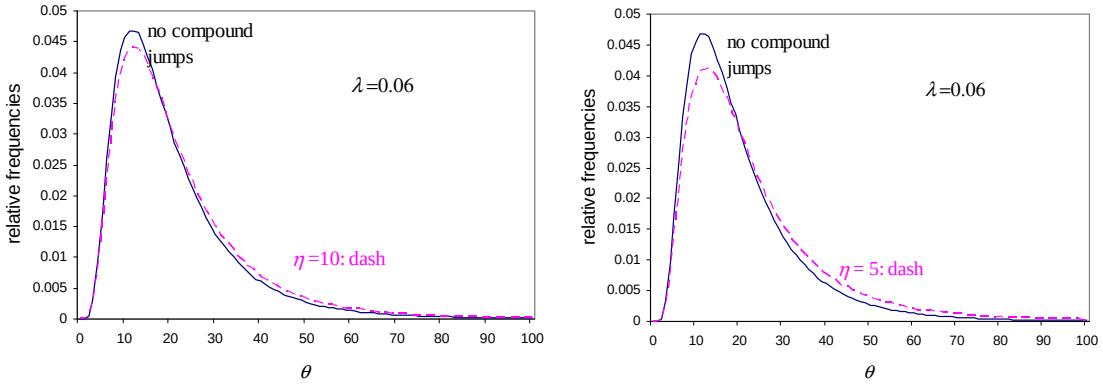

Notes: The probability distribution functions for η = 5 and η = 10 are skewed to the right, and the skewness increases as the value of σ increases. The probability distribution functions start at zero, increase to their modes, and decrease thereafter. The solid curves give the geometrical Brownian motion without compound jumps, i.e. without the last term in (18). The dashed curves give the simulated (lognormal) probability density function with jumps.

The salient features of the distribution are the location of its peak and the shape and extent of the distribution at large θ. The model specification creates positive skewness in the distribution of θ.[11] Figure 1 indicates the predominance of the right fat tail in a transparent way. When comparing the Monte Carlo results with jumps (dashed curves) and without jumps (solid curves), it is apparent that for η = 10 the probability of extreme events occurring is relatively close to the Brownian motion distribution without compound jumps. On the contrary, for η = 5 the distributions are somewhat more stretched out, with more mass in the right tails at the expense of lower modes. One way to reconcile the probability density plots with the data is to calculate the implied probabilities of an extreme event $\theta > \theta^*$. Table 1 presents these implied extreme event probabilities from our Monte Carlo exercise. The period under consideration is 10 years. Due to lack of empirical data, the choice of a baseline parameter for η is somewhat arbitrary. We choose a value of η = 10 in order to be broadly consistent with rough and scant estimates of extreme-impact tail probabilities. We therefore use λ = 0.06 and η = 10 as our back-of-the-envelope baseline tail estimates in what follows.[12]

[11] Roe and Baker (2007) have recently described climate probability distribution functions from the multi-ensemble climatepredition.net experiment with shapes similar to those in Figure 3. Roe and Baker (2009) have shown that this shape of the distribution is not an artefact of the analysis or choice of model parameters but an inevitable consequence of a system in which complex feedbacks among the individual physical processes are substantially positive.

[12] It is understood that the analysis is inevitably subjective because it requires some form of speculation about undesirable fat-tail probabilities. However, the sensitivity analysis below scrutinizes the baseline parameters and thus provides a good grasp of the robustness of the policy implications.

Table 1: Size-Dependent Extreme Event Probabilities for λ = 0.06 in Percent

	No Jumps	$\eta = 10$	$\eta = 5$
$\theta = 40$	8.52	10.43	13.07
$\theta = 50$	4.15	5.35	7.30
$\theta = 60$	2.14	2.88	4.29
$\theta = 70$	1.15	1.61	2.64
$\theta = 80$	0.65	0.94	1.71

Note: The initial θ is 20. Therefore, the row $\theta > 40$ gives the probability of at least one θ doubling after 10 years.

Another parameter which needs to be considered is T_H. The IPCC's fourth assessment report presents various projections computed by different carbon cycle models and we choose four main projections – B2, A1B, A2 and A1F1 – to test the impact of changes of T_H on the thresholds. Armed with the insights from the Monte Carlo exercise, we now use numerical techniques to solve the optimal stopping problem and calibrate the optimal climate policy response for these four projections. The graphs give the critical threshold values $\bar{\theta}$ delimiting the no action area. For $\theta < \bar{\theta}$, it is optimal to wait before adopting a stringent climate policy that imposes large sunk costs on consumers. In contrast, for $\theta \geq \bar{\theta}$ policymakers will incur the cost of emission reduction to reduce temperature. The intended contribution of these exercises is to illustrate how the choice of selected parameters alters the policy implications. Below is the table for the θ thresholds and the corresponding damage thresholds of equation (17):

Table 2: The impacts of various T_H from Projections B2, A1B, A2 and A1F1 on $\bar{\theta}$ and $\bar{D}$

Scenarios	Temperature change since Pre-Industrial Level, T_H *	$\bar{\theta}$	percentage Damage Thresholds $\bar{D}$ in %
B1	2.4	14.48	2.224
B2 or A1T	3.0	6.56	0.860
A1B	3.4	4.86	0.600
A2	4.0	3.44	0.397
A1F1	4.6	2.69	0.295

Note: 0.6 degrees temperature increase is added to the original figures as we use the changes in temperature since the pre-industrial level.

It is shown that different estimates of T_H lead to very different conclusions as to whether or not the policy maker should act immediately. For example, in the B1 scenario the policymaker would only act when the current damage is over 2.2 percent of world GDP. Thus, a rather restrained and reluctant

policy response can be expected. On the contrary, the A2 and A1F1 scenarios lead to immediate actions from the policymakers to act.

By using the above benchmark values of variables, we can then investigate the impacts of changes in parameters on the policy thresholds $\bar{\theta}$. Figure 2 shows the impact of changes in η over the grid $\eta_i \in \{5, 20\}$; Figure 3 shows the impact of changes in λ over the grid $\lambda_i \in \{0.0, 0.12\}$. These numerical assumptions span a broad range of possibilities. The numerical results in Figures 2 and 3 can be interpreted as follows: For smaller values of η, greater disasters happen more often leading to a much lower policy threshold $\bar{\theta}$. This implies that an increasing probability of tail risks sharply strengthens the case for earlier reduction of GHG emissions with more stringent climate policies increasing in fatter tails.[13] Figure 3 indicates the sensitivity of the policy threshold $\bar{\theta}$ with respect to λ. A larger λ implies a larger jump probability. The policy implications are again stark. The numerical results suggest that policymakers need to respond more aggressively to climate change for larger λ, i.e. optimal policies turn out to be significantly more "conservationist". The numerical results also call into question previous work which has neglected such possibilities.

Figure 2: The Impact of Changes in η on the Policy Thresholds θ and D

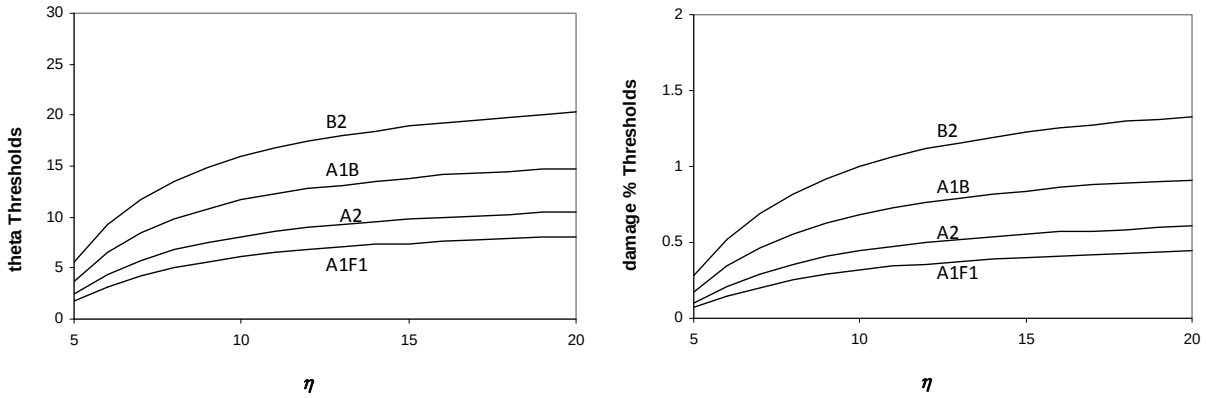

[13] This qualitative result of more drastic GHC reductions as an insurance to hedge tail risks is consistent with the well-known "minimax" strategy in game theory. In these games, the objective is to determine the optimum pay-off for each separate strategy in order to minimize the maximum gain of the opponents. In climate policy, policymakers are not playing a traditional game but a battle against the forces of nature. Under the minimax rule, a strategy must be selected for which the maximum possible damage is as small as possible.

Figure 3: The Impact of Changes in λ on the Policy Threshold θ and D

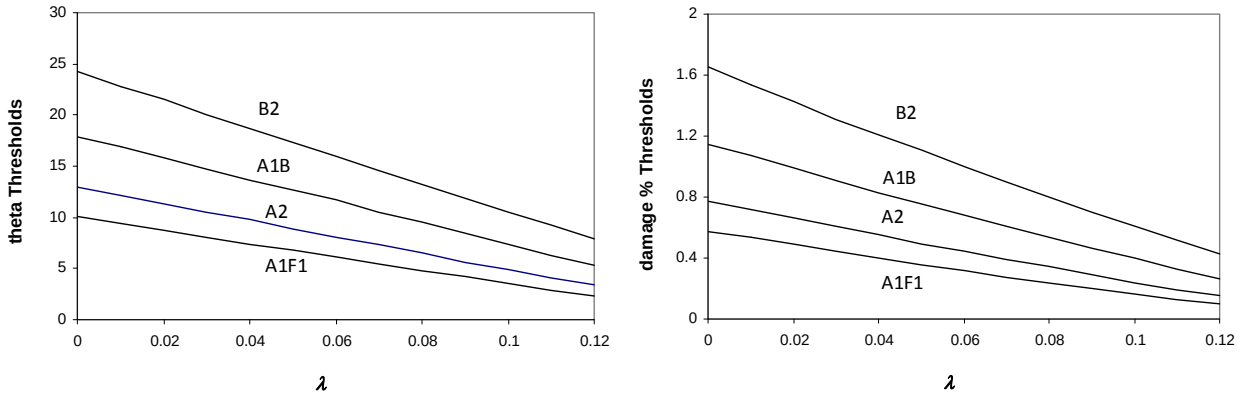

In Figures 2 and 3 we have used a counterfactual – and more pessimistic – scenario of $\lambda = 0.12$ for the jump probability. In order to provide readers with an assessment of the implied risks, we have now calculated the probability density distribution of θ for $\lambda = 0.12$ along the lines of Figure 1 and Table 1. The period under consideration in Table 3 is again 10 years. The comparison between Table 1 and Table 2 shows that extreme events are two to three times more likely for our upper bound $\lambda = 0.12$.

Table 3: Size-Dependent Extreme Event Probabilities for $\lambda = 0.12$ in Percent

	No Jumps	$\eta = 10$	$\eta = 5$
$\theta = 40$	18.33	24.24	30.93
$\theta = 50$	8.52	12.50	18.18
$\theta = 60$	4.15	6.76	11.16
$\theta = 70$	2.14	3.81	7.19
$\theta = 80$	1.15	2.22	4.82

Note: The initial θ_0 is 20. Therefore, the row $\theta > 40$ gives the probability of one θ doubling after 10 years.

Figure 4: Probability Density Distribution of θ for $\lambda = 0.12$ and $\eta = 10$ vs. $\eta = 5$

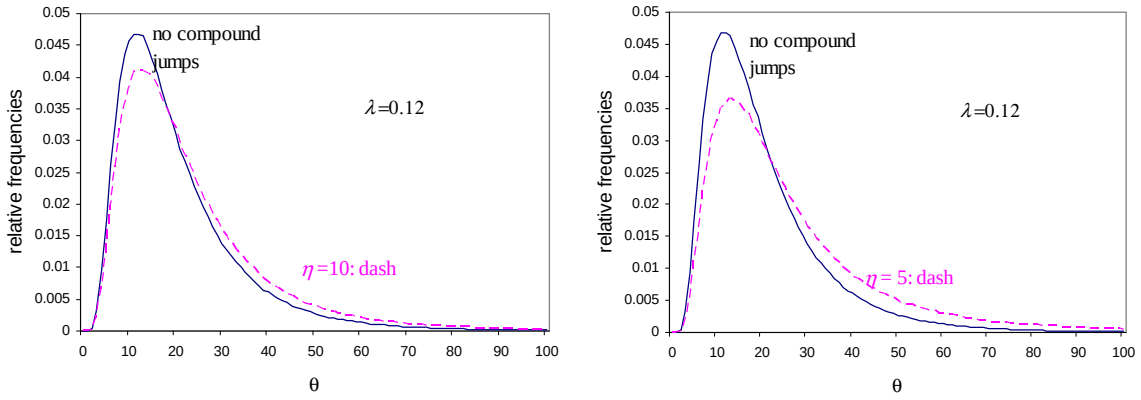

Figure 5 shows the sensitivity of the policy threshold $\bar{\theta}$ to changes in σ. Contrary to standard real option models, $\bar{\theta}$ is not a monotonically increasing function of σ. Rather, the resulting relationship turns out to be hump-shaped. At the outset, an increase in σ implies an increase in the policy threshold $\bar{\theta}$. The more uncertainty there is over the future, the greater is the incentive to wait and see rather than adopting the policy now. Beyond the inflection point, this relationship is inversed. The reason is that in our framework σ also affects the particular solution via θ^{μ}, $\mu > 1$. This effect counteracts, and eventually dominates, the traditional option effect.

Figure 5: The Sensitivity of the Policy Thresholds to Changes in σ

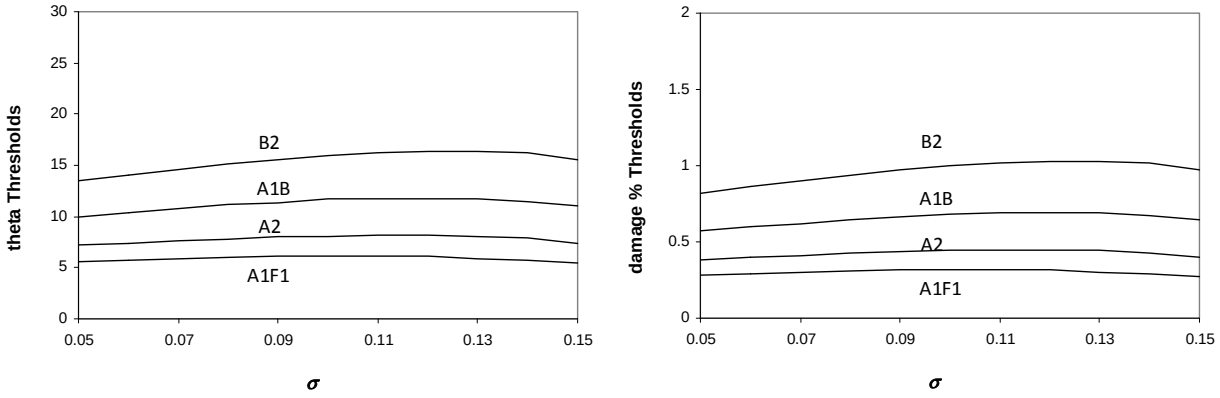

The graph indicates that the impact of second-order (thin-tail) uncertainty is relatively small. The implication is that best-guess or certainty-equivalent climate policy maybe a reasonable approximation. This finding is consistent with findings of Pizer (1999).

Similarly, we can determine the dependence of $\bar{\theta}$ on other parameters. In Figure 6 we investigate how strongly our conclusions would change if we were to adopt a lower discount rate. The Stern Report (2007) represented a break with earlier climate economics modelling approaches in several respects.[14] The most widely discussed innovation was Stern´s (2007) discount rate of just over 1 per cent, which is well outside the consensus range. To explore the sensitivity to alternative discounting assumptions, we employ a range of $0.025 < r < 0.050$. As expected, the results in Figure 6 affirms the view that higher discount rates will bolster the reasons for taking a "wait and see" attitude" towards climate policy. This is because for small r the particular integral is a good deal bigger and therefore the intertemporal damage is substantially larger. Conversely, a higher discounting factor will trigger a later adoption and a lower intensity of climate policy. This highlights the importance of attaining a consensus on the discount rate before an appraisal on the optimal timing of policy implementation can be achieved.

[14] For the discussion of the report, see "Special Topic: The Stern Review Debate" in the journal *Climatic Change* 89 (2008), No. 3-4, pp. 173-449. We don´t consider $r = 0$, i.e. an elimination of the time preference rate [Azar and

Figure 6: The Impact of the Discount Rate *r* on the Policy Thresholds

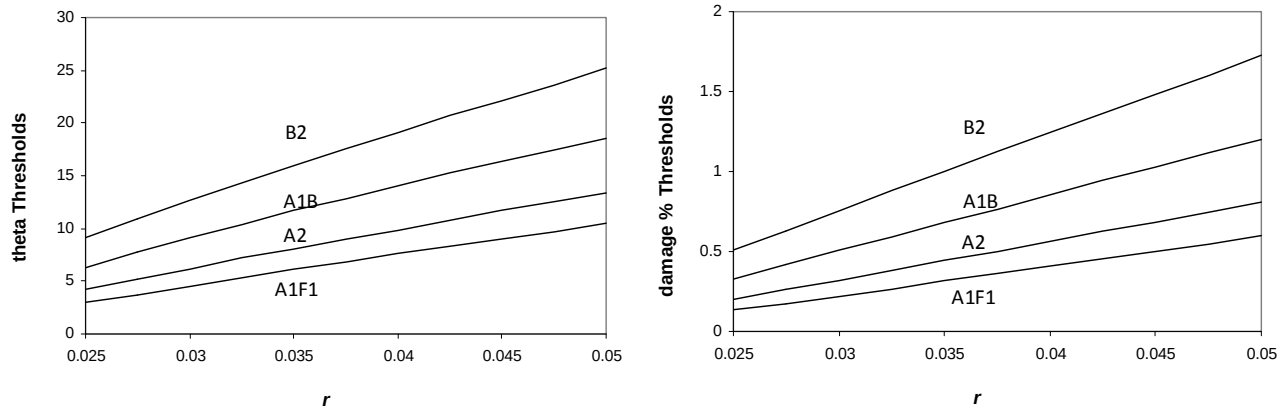

Putting aside the debates over the "correct" values for λ, η, r, and σ, let us finally consider the importance of the damage function exponent μ. How much would optimal policies be changed due to variation in this parameter?

Figure 7: The Impact of μ on the Policy Thresholds

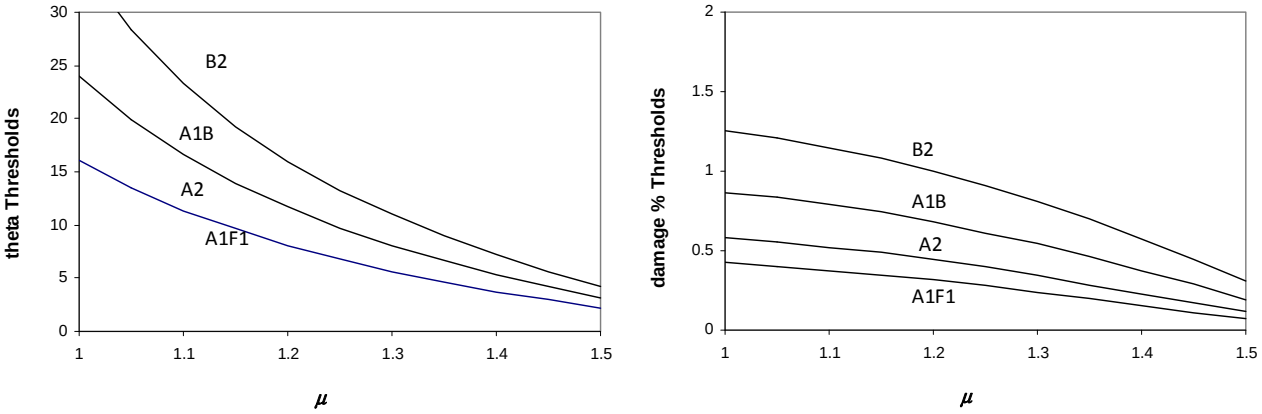

The solution exhibits the properties that one would expect. The effect of μ is stark, far bigger than extreme events parameters themselves. This means that if the extreme events cause convex (much bigger) damages, then governments should act much earlier. However, only with lower parameter values for μ is immediate action motivated. The reason is that exercising the climate policy option incurs large sunk costs, while inaction only involves emissions over the waiting period. The underlying incentive for adopting a "wait and see" stance is that in the future we may receive more data, learn more about climate sensitivity, the economic impact of higher temperatures, and develop low-carbon technologies.

Sterner (1996)] because the particular integral goes to infinity for $r < 0.013$ with current benchmark values and therefore the system explodes.

5. Summary and Conclusions

The possibility of low-probability extreme events calls for a fresh look at the optimal intensity and timing of climate policy. The contribution of this paper is to develop a modelling framework for formally investigating the impact of higher-moment uncertainty on near-term climate policies. More specifically, we specify a continuous-time real option model more general than those used by others, in that it includes low probability extreme events. The numerical calibrations indicate the importance of perhaps unlikely but potentially significant "tail risk". Factoring a fat tail into the real option framework demonstrates a higher value of pre-emptive climate policy.

Although we believe that a hierarchy of models of increasing comprehensiveness will eventually need to be used in order to refine the basic insights we provide here, policymakers should nevertheless actively overcome the common bias towards undervaluing extreme events. In this spirit, the modelling framework can lead policymakers to improve the valuation of climate change that occurs with great uncertainty or low probability and target an important set of low-probability possibilities in a sensible way.

Appendix A: Derivation of Equations (10) and (11)

We need to find the direct integral solution to equation (1) in the text without considering the real options. Substituting equation (3) into the integral of equation (1) yields

$$W = \int_0^\infty e^{-\eta_Y t}\left(1 - k\theta_t^\mu e^{-2\frac{\ln 2}{H}t}\left(T - 2T_H\left(1 - e^{\frac{\ln 2}{H}t}\right)\right)^2\right)e^{-(r-\eta_Y)t}dt$$

$$\text{(A1)} \qquad = \int_0^\infty e^{-(r-\eta_Y)t}dt - k\left(4T_H^2 - 4TT_H + T^2\right)\int_0^\infty \theta_t^\mu e^{-\left(r+2\frac{\ln 2}{H}-\eta_Y\right)t}dt$$

$$+ 4k\left(2T_H^2 - T_H T\right)\int_0^\infty \theta_t^\mu e^{-\left(r+\frac{\ln 2}{H}-\eta_Y\right)t}dt - 4kT_H^2\int_0^\infty \theta_t^\mu e^{-(r-\eta_Y)t}dt$$

Collecting terms gives

$$\text{(A2)} \qquad W = \int_0^\infty e^{-(r-\eta_Y)t}dt - k\left(4T_H^2 - 4TT_H + T^2\right)\int_0^\infty \theta_t^\mu e^{-\left(r+2\frac{\ln 2}{H}-\eta_Y\right)t}dt$$

$$+ 4k\left(2T_H^2 - T_H T\right)\int_0^\infty \theta_t^\mu e^{-\left(r+\frac{\ln 2}{H}-\eta_Y\right)t}dt - 4kT_H^2\int_0^\infty \theta_t^\mu e^{-(r-\eta_Y)t}dt.$$

Most of the above integrals involve general forms of the integral

$$\text{(A3)} \qquad \int_0^\infty \theta_t^a e^{-bt}dt \text{, subject to } d\theta_t = \alpha_0\theta_t dt + \sigma\theta_t dz_t + \theta_t dX_t.$$

A natural way to solve the above integral is via the Bellman equation,

(A4) $$bV = \theta^a + \alpha\theta V_\theta + \frac{1}{2}\sigma^2\theta^2 V_{\theta\theta} + \int_{-\infty}^{\infty}\left[V\left(\theta e^y\right) - V\left(\theta\right)\right]\nu\left(dy\right).$$

We conjecture that V under the Levy process setting have the following form of solution,

(A5) $$V = c\theta^\mu,$$

where c is an unknown parameter to be determined. We then have

(A6) $$\alpha a\theta^a V_\theta = c\alpha a\theta^a$$

and

(A7) $$\frac{1}{2}\sigma^2\theta^2 V_{\theta\theta} = \frac{1}{2}c\sigma^2 a\left(a-1\right)\theta^a.$$

The Levy integral term of V needs to be handled with care. As V is drawn from two separate cases, one can compute the integral of $\lambda\int_0^\infty\left[W\left(\theta e^y\right) - W\right]\eta e^{-\eta y}dy$ without considering changes of states for exponential compound jumps involved in real options.

(A8) $$\lambda\left[\int_0^\infty\left[c\theta^a e^{ay} - c\theta^a\right]\eta e^{-\eta y}dy\right] = \lambda\eta c\theta^a M\left(\frac{1}{\eta-a} - \frac{1}{\eta}\right) = \lambda c\theta^a M\frac{a}{\eta-a},$$

where the constraint $\eta > a$ is needed to avoid the infinity of the integral. Substituting equations (A6)-(A8) back to equation (A4) yields

(A9) $$cb\theta^a M = \theta^a + c\alpha a\theta^a + \frac{1}{2}ca\left(a-1\right)\sigma^2\theta^a + \frac{\lambda ac\theta^a}{\eta-a}.$$

Rearranging the above equation gives

(A10) $$\theta^a\left(c\left(b - \alpha a - \frac{1}{2}a\left(a-1\right)\sigma^2 - \frac{\lambda a}{\eta-a}\right) - 1\right) = 0.$$

It is a straightforward to show that the solutions to $\int_0^\infty \theta_t^a e^{-bt}dt$ are represented by

(A11) $$V = \frac{\theta^a}{b - \alpha a - \frac{1}{2}a\left(a-1\right)\sigma^2 - \frac{\lambda a}{\eta-a}}.$$

Now we can substituting (A11) back to (A2) by setting w = 0 prviding the value of no action

(A12) $$W^{\mathrm{N}} = \frac{1}{\left(r-\eta_Y\right)} - k\left[\frac{\left(2T_H - T\right)^2}{\phi_1 + 2\frac{\ln 2}{H}} - \frac{4T_H\left(2T_H - T\right)}{\phi_1 + \frac{\ln 2}{H}} + \frac{4T_H^2}{\phi_1}\right]\theta^\mu,$$

where $\phi_1 = r - \eta_Y - \mu\alpha - \frac{1}{2}\mu\left(\mu-1\right)\sigma^2 - \frac{\lambda\mu}{\eta-\mu} > 0$.

Following the same reasoning, we obtain the value of taking action by replacing T_H with τ.

$$\text{(A13)}\quad W^{\mathrm{A}} = (1-w)\left(\frac{1}{(r-\eta_Y)} - k\left[\frac{(2\tau - T)^2}{\phi_1 + 2\frac{\ln 2}{H}} - \frac{4\tau(2\tau - T)}{\phi_1 + \frac{\ln 2}{H}} + \frac{4\tau^2}{\phi_1} \right] \theta^{\mu} \right),$$

Note that terms in the brackets [.] of equations (A12) and (13) can be show as positive, since

$$\begin{aligned}
&\frac{(2T_H - T)^2}{\phi_1 + 2\frac{\ln 2}{H}} - \frac{4T_H(2T_H - T)}{\phi_1 + \frac{\ln 2}{H}} + \frac{4T_H^2}{\phi_1} \\
&= \frac{(2T_H - T)^2}{\phi_1 + \frac{\ln 2}{H}} - \frac{4T_H(2T_H - T)}{\phi_1 + \frac{\ln 2}{H}} + \frac{4T_H^2}{\phi_1 + \frac{\ln 2}{H}} + \frac{(2T_H - T)^2}{\phi_1 + 2\frac{\ln 2}{H}} - \frac{(2T_H - T)^2}{\phi_1 + \frac{\ln 2}{H}} - \frac{4T_H^2}{\phi_1 + \frac{\ln 2}{H}} + \frac{4T_H^2}{\phi_1} \\
&= \frac{T^2}{\phi_1 + \frac{\ln 2}{H}} + \frac{4T_H^2 \frac{\ln 2}{H}}{\phi_1\left(\phi_1 + \frac{\ln 2}{H}\right)} - \frac{\frac{\ln 2}{H}(2T_H - T)^2}{\left(\phi_1 + \frac{\ln 2}{H}\right)\left(\phi_1 + 2\frac{\ln 2}{H}\right)} \\
&= \frac{T^2}{\phi_1 + \frac{\ln 2}{H}} + \frac{4T_H^2 \frac{\ln 2}{H}}{\phi_1\left(\phi_1 + \frac{\ln 2}{H}\right)} - \frac{4T_H^2 \frac{\ln 2}{H}}{\left(\phi_1 + \frac{\ln 2}{H}\right)\left(\phi_1 + 2\frac{\ln 2}{H}\right)} + \frac{\frac{\ln 2}{H}(4T_H T - T^2)}{\left(\phi_1 + \frac{\ln 2}{H}\right)\left(\phi_1 + 2\frac{\ln 2}{H}\right)}.
\end{aligned}$$

Then finally, we have

$$\begin{aligned}
&\frac{(2T_H - T)^2}{\phi_1 + 2\frac{\ln 2}{H}} - \frac{4T_H(2T_H - T)}{\phi_1 + \frac{\ln 2}{H}} + \frac{4T_H^2}{\phi_1} \\
&= \frac{T^2}{\phi_1 + \frac{\ln 2}{H}} + \frac{8\left(\frac{\ln 2}{H}\right)^2 T_H^2}{\phi_1\left(\phi_1 + \frac{\ln 2}{H}\right)\left(\phi_1 + 2\frac{\ln 2}{H}\right)} + \frac{\frac{\ln 2}{H}(4T_H - T)T}{\left(\phi_1 + \frac{\ln 2}{H}\right)\left(\phi_1 + 2\frac{\ln 2}{H}\right)} > 0.
\end{aligned} \quad \text{(A14)}$$

Similarly for the square bracket term of equation (A13)

$$\begin{aligned}
&\frac{(2\tau - T)^2}{\phi_1 + 2\frac{\ln 2}{H}} - \frac{4\tau(2\tau - T)}{\phi_1 + \frac{\ln 2}{H}} + \frac{4\tau^2}{\phi_1} \\
&= \frac{T^2}{\phi_1 + \frac{\ln 2}{H}} + \frac{8\left(\frac{\ln 2}{H}\right)^2 \tau^2}{\phi_1\left(\phi_1 + \frac{\ln 2}{H}\right)\left(\phi_1 + 2\frac{\ln 2}{H}\right)} + \frac{\frac{\ln 2}{H}(4\tau - T)T}{\left(\phi_1 + \frac{\ln 2}{H}\right)\left(\phi_1 + 2\frac{\ln 2}{H}\right)} > 0.
\end{aligned} \quad \text{(A15)}$$

Thus, it is obvious that $F(T) > 0$ for equation (13) in the text

(A16) $$F(T)=\frac{wT^2}{\phi_1+\frac{\ln 2}{H}}+\frac{8\left(\frac{\ln 2}{H}\right)^2\left(T_H^2-(1-w)\tau^2\right)}{\phi_1\left(\phi_1+\frac{\ln 2}{H}\right)\left(\phi_1+2\frac{\ln 2}{H}\right)}+\frac{\frac{\ln 2}{H}\left(\left(4T_H-T\right)T-(1-w)(4\tau-T)T\right)}{\left(\phi_1+\frac{\ln 2}{H}\right)\left(\phi_1+2\frac{\ln 2}{H}\right)}>0.$$

Appendix B: Computation of Real Options by Explicit Finite Difference Method

The integro-differential Bellman equation for real options can be represented by the homogenous part of equation (9) in the text,

(B1) $$rW^{\mathrm{O}}=\frac{\ln(2)}{H}(2T_H-T)W_T^{\mathrm{O}}+\alpha\theta W_\theta^{\mathrm{O}}+\frac{1}{2}\sigma^2\theta^2W_{\theta\theta}^{\mathrm{O}}+\lambda\int_0^\infty\left[W\left(\theta e^y\right)-W(\theta)\right]\eta e^{-\eta y}dy.$$

By using an explicit finite difference method, we obtain the following approximations,

(B2) $$\frac{\partial W^{\mathrm{O}}}{\partial\theta}=\frac{v_{i+1,j+1}-v_{i+1,j-1}}{2\Delta X},$$

(B3) $$\frac{\partial^2W^{\mathrm{O}}}{\partial\theta^2}=\frac{v_{i+1,j+1}+v_{i+1,j-1}-2v_{i+1,j}}{\Delta X^2},$$

(B4) $$\frac{\partial W^{\mathrm{O}}}{\partial T}=\frac{v_{i+1,j}-v_{i,j}}{\Delta T},$$

We follow the approximation by Cont and Voltchkova (2005) for $\lambda\int_0^\infty\left[W\left(\theta e^y\right)-W(\theta)\right]\eta e^{-\eta y}dy$.

(B5) $$\lambda\int_0^\infty\left[W\left(\theta e^y\right)-W(\theta)\right]\eta e^{-\eta y}dy=\sum_{k=K_d}^{K_u}\nu_k\left(v_{i+1,j+k}-v_{i+1,j}\right).$$

For normalised $j\Delta X$ = 1, we have $\nu_k=\int_{(k-1/2)\Delta X}^{(k+1/2)\Delta X}\nu(y)\quad=-\lambda\left(e^{-\eta(k+1/2)\Delta X}-e^{-\eta(k+1/2)\Delta X}\right)$ $=\lambda\left(e^{-\eta(k-1/2)\Delta X}-e^{-\eta(k+1/2)\Delta X}\right)$. Therefore, we have

(B6) $$\nu_k=\lambda\left(e^{-\frac{\eta(k-1/2)\Delta X}{j\Delta X}}-e^{-\frac{\eta(k+1/2)\Delta X}{j\Delta X}}\right).$$

Substituting equations (B2) – (B5) back into equation (B1) yields

(B7) $$\begin{aligned}rv_{i,j}=&\alpha j\Delta X\left(\frac{v_{i+1,j+1}-v_{i+1,j-1}}{2\Delta X}\right)+\frac{1}{2}\sigma^2j^2\Delta X^2\left(\frac{v_{i+1,j+1}+v_{i+1,j-1}-2v_{i+1,j}}{\Delta X^2}\right)\\&+\left(2\frac{\ln(2)}{H}T_H-\frac{\ln(2)}{H}i\Delta T\right)\left(\frac{v_{i+1,j}-v_{i,j}}{\Delta T}\right)+\sum_{k=K_d}^{K_u}\nu_k\left(v_{i+1,j+k}-v_{i+1,j}\right).\end{aligned}$$

Finally, rearranging and simplifying further allows us to obtain

(B8) $$v_{i,j} = a^*_{i,j} v_{i+1,j-1} + b^*_{i,j} v_{i+1,j} + c^*_{i,j} v_{i+1,j+1} + d^*_{i,j} \sum_{k=K_d}^{K_u} \nu_k \left(v_{i+1,j+k} - v_{i+1,j} \right),$$

where

$$a^*_{i,j} = \frac{1}{2\frac{\ln(2)}{H} T_H + \left(r - \frac{\ln(2)}{H} i \right) \Delta T} \left(\frac{1}{2} \sigma^2 j^2 \Delta T - \frac{1}{2} \alpha j \Delta T \right),$$

$$b^*_{i,j} = \frac{1}{2\frac{\ln(2)}{H} T_H + \left(r - \frac{\ln(2)}{H} i \right) \Delta T} \left(\beta E - \delta i \Delta T - \sigma^2 j^2 \Delta T \right),$$

$$c^*_{i,j} = \frac{1}{2\frac{\ln(2)}{H} T_H + \left(r - \frac{\ln(2)}{H} i \right) \Delta T} \left(\frac{1}{2} \alpha j \Delta T + \frac{1}{2} \sigma^2 j^2 \Delta T \right),$$

$$d^*_{i,j} = \frac{\Delta T}{2\frac{\ln(2)}{H} T_H + \left(r - \frac{\ln(2)}{H} i \right) \Delta T},$$

Note that $2\frac{\ln(2)}{H} T_H + \left(r - \frac{\ln(2)}{H} i \right) \Delta T$ need to be positive; otherwise, the scheme does not converge.

Next we need to decide the free boundary conditions for threholds $\bar{\theta}$, as well as the boundary and terminal conditions for θ and T. The boundary and terminal conditions of equations (14) – (16) become

(B9) $$v_{i,j=0} = 0,$$

(B10) $$v_{i,j_{\max}} = \max\left(W^{\mathrm{A}}_{i,j_{\max}} - W^{\mathrm{N}}_{i,j_{\max}}, 0 \right),$$

(B11) $$v_{i_{\max},j} = \max\left(W^{\mathrm{A}}_{i_{\max},j} - W^{\mathrm{N}}_{i_{\max},j}, 0 \right),$$

where

(B12) $$W^{\mathrm{N}}_{i,j} = \frac{1}{(r - \eta_Y)} - k \left[\frac{\left(2T_H - i\Delta T \right)^2}{\phi_1 + 2\frac{\ln 2}{H}} - \frac{4T_H \left(2T_H - i\Delta T \right)}{\phi_1 + \frac{\ln 2}{H}} + \frac{4T_H^2}{\phi_1} \right] (j\Delta X)^{\mu},$$

(B13) $$W^{\mathrm{A}}_{i,j} = (1-w) \left(\frac{1}{(r - \eta_Y)} - k \left[\frac{\left(2\tau - i\Delta T \right)^2}{\phi_1 + 2\frac{\ln 2}{H}} - \frac{4\tau \left(2\tau - i\Delta T \right)}{\phi_1 + \frac{\ln 2}{H}} + \frac{4\tau^2}{\phi_1} \right] (j\Delta X)^{\mu} \right).$$

The numerical solutions for the real options start backwards from terminal condition B(10) at $i_{\max}$ with boundary conditions (B9) and (B10) and free boundary conditions checked. Afterwards, we step backwards to $i_{\max} - 1$ and compute $v_{i_{\max}-1,j}$, and the free boundary conditions – the value-matching condition – becomes

(B13) $v_{i,j} = \max\left(W_{i,j}^{\mathrm{A}} - W_{i,j}^{\mathrm{N}}, v_{i,j}\right)$.

After having obtained the thresholds for θ, the backward procedure is used until $i\Delta T = 0.6$, the currrent level of *T*, is obtained.

References:

Azar, C., Sterner, T. (1996) "Discounting and Distributional Considerations in the Context of Global Warming", *Ecological Economics* 19, 169–185.

Baranzini A., Chesney M., Morisset J. (2003) "The Impact of Possible Climate Catastrophes on Global Warming Policy", *Energy Policy*, 31, 691–701.

Box, G.E.P. and M.E. Muller (1958) "A Note on the Generation of Random Normal Deviates", *Annals Mathematical. Statistics* 29, 610-611.

Chevalier-Roignant, B., Flath, C. M., Huchzermeier, A., and L. Trigeorgis (2011) "Strategic Investment Under Uncertainty: A Synthesis", *European Journal of Operational Research* 215, 639-650.

Cont, R. and P. Tankov (2004) *Financial Modelling with Jump Processes*, London (Chapman & Hall).

Cont, R. and E. Voltchkova (2005) "A Finite Difference Scheme for Option Pricing in Jump-Diffusion and Exponential Levy Models", SIAM J. Numer. Anal. 43, 1596-1626.

Dietz, S. and N. Stern (2008) "Why Economic Analysis Supports Strong Action on Climate Change: A Response to the Stern Review´s Critic´s", *Review of Environmental Economics and Policy* 2, 94-113.

Dixit, A. and R.S. Pindyck (1994) *Investment Under Uncertainty*, Princeton (Princeton University Press).

Hoyos, C.D., Agudelo, P.A., Webster, P.J. and J.A. Curry (2006) "De-Convolution of the Factors Contributing to the Increase in Global Hurricane Intensity", *Science* 312, 94-97.

Intergovermental Panel on Climate Change (2008) *Climate Change 2007: Impacts, Adaptation and Vulnerability*, Cambridge (Cambridge University Press).

Kou, S. G. and H. Wang (2004) "Option Pricing Under a Double Exponential Jump Diffusion Model", Management Science 50, 1178-1192.

Maslin, M. and P. Austin (2012) "Climate Models at Their Limit", *Nature* 486, 183-184.

Martzoukos, S.H. and L. Trigeorgis (2002) "Real (Investment) Options with Multiple Sources of Rare Events", *European Journal of Operational Research* 136, 696-706

Oksendal, B. and A. Sulem (2007) *Applied Stochastic Control of Jump Diffusions*, 2nd edition, Berlin & New York (Springer).

Pindyck, R.S. (2000) "Irreversibilities and the Timing of Environmental Policy", *Resource and Energy Economics* 22, 233-259.

Pindyck, R.S. (2007) "Uncertainty in Environmental Economics", *Review of Environmental Economics and Policy* 1, 45-65.

Pizer, W.A. (1999) “The Optimal Choice of Climate Change Policy in the Presence of Uncertainty”, *Resource and Energy Economics* 21, S. 255-287

Rachev, S. T. (2003) *Handbook of Heavy Tailed Distributions in Finance: Handbooks in Finance*, Amsterdam (North Holland).

Roe, G.H. and M.B. Baker (2007) “Why is Climate Sensitivity So Unpredictable?”, *Science* 318, 26 October 2009, 629-632.

Stern, N. (2007) *The Economics of Climate Change - The Stern Review*, Cambridge (Cambridge University Press).

Schoutens, W. (2003) *Levy Processes in Finance: Pricing Financial Derivatives*, Oxford (Wiley & Blackwell).

Sato, K. (1999) *Levy Processes and Infinitely Divisible Distributions*, Cambridge University Press, Cambridge, UK.

Stokey, N.L. (2008) *The Economics of Inaction: Stochastic Control Models with Fixed Costs*. Princeton (Princeton University Press).

Tol, R. (2009) “The Economic Effects of Climate Change”, *Journal of Economic Perspectives* 23, 29-51.

Valdes, P. (2011) “Built for Stability”, *Nature Geosciences* 4, 414-416.

Webster, P.J., Holland, G.J., Curry, J.A. and H.-R. Chang (2005) “Changes in Tropical Cyclone Number, Duration, and Intensity in a Warming Environment”, *Science* 309, 1844-1846.

Weitzman, M. (2009) “On Modeling and Interpreting the Economics of Catastrophic Climate Change”, *The Review of Economics and Statistics* 91, 1-19.

Weitzman, M. (2010) “What is the “Damages Function” for Global Warming – and What Difference might it Make?”, *Climate Change Economics* 1, 57–69.